Perfectly matched transmission problem with absorbing layers : application to anisotropic acoustics in convex polygonal domains

Edouard Demaldent, Sébastien Imperiale

Perfectly matched transmission problem with absorbing layers : application to anisotropic acoustics in convex polygonal domains

E. Demaldent[1*], S. Imperiale[12*]

[1] *CEA, LIST, 91191 Gif-sur-Yvette CEDEX, FRANCE*
[2]*INRIA Rocquencourt, POems, domaine de Voluceau, B. P. 105 78153 Le Chesnay, FRANCE*

SUMMARY

This paper presents an original approach to design perfectly matched layers (PML) for anisotropic scalar wave equations. This approach is based, first, on the introduction of a modified wave equation and, second, on the formulation of general "perfectly matched" transmission conditions for this equation. The stability of the transmission problem is discussed by way of the adaptation of a high frequency stability (necessary) condition, and we apply our approach to construct PML suited for any convex domain with straight boundaries. A new variational formulation of the problem, including a Lagrange multiplier at the interface between the physical and the absorbing domains, is then set and numerical results are presented in 2D and 3D. These results show the efficiency of our approach when using constant damping coefficients combined with high order elements. Copyright © 0000 John Wiley & Sons, Ltd.

1. INTRODUCTION

This paper regards the study of perfectly matched layers (PML) [1] for time-dependent scalar anisotropic wave equations in convex polygonal domains. The PML technology is often used to model unbounded homogeneous domains in wave propagation simulations. It consists in surrounding a bounded (possibly inhomogeneous) domain of interest Ω_φ, that may include source terms or initial data, by layers in which the wave equation is modified in order to obtain an exponential decrease of energy (see figure 1 for a schematic of a domain). It is said to be perfectly matched when no reflection occurs at the interface between the (physical) domain of interest and the (absorbing) layers. Compared to the use of absorbing boundary conditions (ABC), PML are commonly considered to be more accurate than low-order ABC and easier to implement than high-order ones.

The absorbing behavior of the equation stated in PML is described by a damping function which is introduced through a change of variables in the harmonic regime. The main difficulty lies in designing a change of variables that ensures perfectly matched properties as well as stability and damping properties. The resulting problem is written back in the time domain by splitting the unknown (the solution is expressed by the sum of solutions of transport equations which involve only one spatial derivative) or by adding auxiliary variables (see [2, 3] for instance). Each method has its own advantages and drawbacks (the use of auxiliary variables may yield PML that are adapted to some nonlinear media for example [4]). To our knowledge no comparative study on the different

---

[*]Correspondence to: edouard.demaldent@cea.fr, sebastien.imperiale@inria.fr
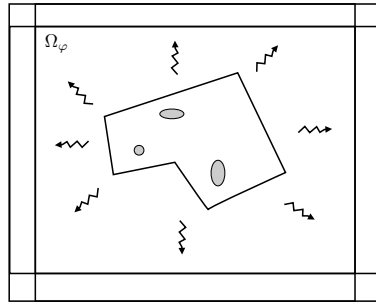
Figure 1. Domain of interest Ω_φ surrounded by absorbing layers.

formulations of the PML has shown the superiority of one formulation on the others. In this paper we focus on the splitting approach as introduced originally by [1], [5] and [6] because of its ease of implementation.

However, when considering efficiency, it is better to preserve the (unsplit) wave equation in the physical domain when coupling it with the split absorbing domain and to use conformal elements, to limit the number of unknowns. Most of the implementations use a damping function which is null at the interface of the physical domain and the PML which simplifies the discretization of the underlying transmission problem. Compared to the use of a constant damping function (which simplifies the implementation), this results in larger absorbing layers and thereby to additional computational costs. Besides, we have not found in existing literature a proper variational formulation of the full transmission problem, when the split perfectly matched layers are coupled with the unsplit wave equation then discretized by conformal elements.

The approach we propose follows the approach first introduced by [7] for the construction of the PML using complex change of variables and [8] for the stability analysis. The PML are constructed at a continuous level then discretized. A recent alternative suggests to construct the layers at a discrete level using mid-point quadrature and shows that they are perfectly matched to the continuous physical problem [9]. This work has been extended to anisotropic acoustics in rectangular domains [10]. Although promising to deal with convex polygonal geometries, we will not follow this approach and we will show that PML can be set at the continuous level for time-dependent scalar anisotropic wave equations in convex polygonal domains.

A primary reason for the novelty of this paper lies in its interpretation of the damped equations as wave equations with complex coefficients which enable us to design perfectly matched layers through the statement of some explicit transmission conditions at the interface between the physical and the absorbing domains. The necessary stability conditions stated in [8] are then adapted to our case. A second reason for the originality of this paper is the use of a (non-overlapping) Mortar element [11, 12] technique to write the variational form of the transmission problem. This allows the use of a constant damping function, while the second order unsplit wave equation is preserved in the physical domain, and thereby decreases the computational costs. Finally, we detail the construction of PML for anisotropic acoustic waves (with a technique similar to what is done in [7] and [13] but that handles corners in 2d and 3d) and numerical results (in 2d and 3d) show that a single layer of high-order elements (like those presented in [14]) is sufficient in the PML to obtain a good absorption and low reflections.

The paper is organized as follows. The study of perfectly matched layers in the harmonic regime is done in section 2 and the practical construction of PML for anisotropic and convex polygonal domains is dealt in section 3; the splitting as well as the time-dependent discrete scheme are developed in section 4 while numerical results are presented in section 5. More precisely, after a brief recap of the main features of the wave equation in section 2.1, we start from the classical PML change of variable to introduce a class of media whose (possibly complex) coefficients depend on the frequency in section 2.2. Then, in section 2.3, we focus on the transmission/reflection phenomena that arise when two different (frequency dependent) media are juxtaposed (the half space problem). In particular, we give sufficient conditions (using specific transmission equations) for the existence

of a plane wave solution that is transmitted without reflection. This study is extended to the full space problem (*i.e.* corner regions are handled) in section 2.4 and the high frequency stability necessary condition stated in [8] is extended to our case in section 2.5. Then in section 3, which represents the core section of this article, we use the tools previously introduced to construct PML for anisotropic media in convex polyhedral domain. The split formulation, which is inspired from the one introduced in [1] for Maxwell equations and in [6] for elastodynamic equations, is introduced then extended to the transmission problem in section 4.1. Mortar elements are then introduced in section 4.2 to handle the corresponding weak formulation and the associated discretization scheme is developed.

2. TRANSMISSION PROBLEMS FOR PERFECTLY MATCHED LAYERS IN THE FREQUENCY DOMAIN

Perfectly matched layers are classically interpreted as a change of variable in the frequency domain [5]. After a brief introduction to the scalar anisotropic wave equation in section 2.1, we start from this interpretation to build a class of media in section 2.2 obtained by a change of variables, whose (possibly complex) coefficients depend on the frequency. The transmission/reflection phenomena that arise when two different media of this class are juxtaposed is studied in section 2.3. In particular, we give sufficient conditions for the existence of a plane wave solution that is transmitted without reflection. Then we focus on the treatment of corner domains in section 2.4. Finally, the necessary high frequency stability condition (HFS) stated in [8] is extended to our class of media in section 2.5.

2.1. Scalar anisotropic wave equation and dispersion relation

We consider the scalar anisotropic wave equation in time domain and in the whole space $\mathbb{R}^d$, where $d = 2$ or 3 is the dimension:

$$
\begin{cases}
\dfrac{\partial^2}{\partial t^2} u(\mathbf{x}, t) - \nabla \cdot A \, \nabla u(\mathbf{x}, t) = f(\mathbf{x}, t) & \forall \, (\mathbf{x}, t) \, \in \mathbb{R}^d \times \mathbb{R}^+, \\[2mm]
u(\mathbf{x}, 0) = u^0(\mathbf{x}), \quad \dfrac{\partial}{\partial t} u(\mathbf{x}, 0) = u^1(\mathbf{x}), & \forall \, \mathbf{x} \in \mathbb{R}^d,
\end{cases}
\tag{1}
$$

with $\mathbf{x} = [x_1, \cdots, x_d]^T$, $\nabla = [\partial/\partial x_1, \cdots, \partial/\partial x_d]^T$ and where A is a $d \times d$ real matrix satisfying the following symmetry and positivity property.

Assumption 1
The matrix A is symmetric definite positive. Hence the scalar $a(\mathbf{k})$ defined by

$$
a(\mathbf{k}) = \sum_{i,j=1}^{d} [A]_{ij} [\mathbf{k}]_i [\mathbf{k}]_j
\tag{2}
$$

is strictly positive for all $\mathbf{k} \in \mathbb{R}^d \setminus \{0\}$.

We assume that the source term f and initial data (u^0 and u^1) have compact support in a bounded and convex set $\Omega_\varphi \subset \mathbb{R}^d$, called domain of interest, and that A is constant in $\overline{\mathbb{R}^d \setminus \Omega_\varphi}$. Outside this domain of interest, we thus consider the homogeneous equation (for a homogeneous medium)

$$
\frac{\partial^2}{\partial t^2} u - \nabla \cdot A \, \nabla u = 0.
\tag{3}
$$

It is well known that solutions of (3) are a combination of plane waves of the form

$$
u(\mathbf{x}, t) = u_0 \, e^{\imath(\omega(\mathbf{k})t - \mathbf{k} \cdot \mathbf{x})}
\tag{4}
$$

where u_0 is a complex scalar and $\mathbf{k} \in \mathbb{R}^d \setminus \{0\}$ is the wave vector. The function $\omega(\mathbf{k})$ is solution of the so called dispersion relation

$$F(\omega, \mathbf{k}) = \omega^2(\mathbf{k}) - a(\mathbf{k}) = 0, \tag{5}$$

Classically one defines the group velocity

$$V(\mathbf{k}) = \nabla_{\mathbf{k}}\omega(\mathbf{k}) = -\big(\frac{\partial}{\partial \omega} F(\omega, \mathbf{k})\big)^{-1} \nabla_{\mathbf{k}} F(\omega, \mathbf{k}) = a(\mathbf{k})^{-1/2} A\mathbf{k}.$$

We also introduce the phase velocity $\mathcal{V}$, the unit propagation direction $\mathbf{K} \in \mathbb{S}^d := \{\mathbf{K} \in \mathbb{R}^d$ such that $|\mathbf{K}| = 1\}$ and the slowness vector S defined by

$$\mathcal{V}(\mathbf{k}) = \frac{\omega(\mathbf{k})}{|\mathbf{k}|}, \quad \mathbf{K} = \frac{\mathbf{k}}{|\mathbf{k}|}, \quad S(\mathbf{k}) = \frac{\mathbf{k}}{\omega(\mathbf{k})} = a(\mathbf{k})^{-1/2}\mathbf{k},$$

and point out that, by homogeneity,

$$F(\omega, \mathbf{k}) = F(\mathcal{V}, \mathbf{K}), \quad S(\mathbf{k}) = S(\mathbf{K}), \quad V(\mathbf{k}) = V(\mathbf{K}).$$

2.2. Definition of propagative media from change of variables

The equation (3) is given in the frequency domain by a Fourier-Laplace transform as

$$-\omega^2\,\hat{u} - \nabla \cdot A\,\nabla\hat{u} = 0, \quad \forall\,\mathbf{x} \in \mathbb{R}^d. \tag{6}$$

Let $D(\omega)$ be a $d \times d$ complex invertible matrix $\forall\,\omega \in \mathbb{R} \setminus \{0\}$. By applying the constant change of variable $\mathbf{x} \leftarrow D\mathbf{x}$ to (6) we obtain the equation

$$-\omega^2\,\hat{u} - \nabla \cdot D^{-1}(\omega)\,A\,D^{-T}(\omega)\,\nabla\hat{u} = 0, \quad \forall\,\mathbf{x} \in \mathbb{R}^d, \tag{7}$$

which can be interpreted as a generalization of (6) to the complex medium characterized by the complex coefficients

$$\tilde{A} = D^{-1}AD^{-T}. \tag{8}$$

This motivates the following definition.

Definition 1
A medium is defined by a set of two $d \times d$ complex matrices denoted by $(A\,;\,D(\omega))$ where $D(\omega)$ is invertible $\forall\,\omega \in \mathbb{R} \setminus \{0\}$. Two media $(A\,;\,D(\omega))$ and $(B\,;\,E(\omega))$ are said to be equivalent if and only if

$$D(\omega)^{-1}AD(\omega)^{-T} = E(\omega)^{-1}BE(\omega)^{-T} \quad \forall\,\omega \in \mathbb{R} \setminus \{0\}.$$

Using (8) and the previous definition, we obviously have $(A\,;\,D(\omega)) \equiv (\tilde{A}(\omega)\,;\,I)$. Solutions of (7) are a combination of plane waves

$$\hat{u}(\mathbf{x}, \omega) = u_0(\omega)e^{-\imath\mathbf{k}\cdot\mathbf{x}}, \quad 1 \le i \le n, \tag{9}$$

for which $\mathbf{k}$ is solution of the modified dispersion relation

$$\tilde{F}(\omega, \mathbf{k}) = F(\omega, D(\omega)^{-T}\mathbf{k}) = 0. \tag{10}$$

2.3. Perfectly matched transmission problem between two media

In the following we assume that the space is split into two subdomains

$$\begin{aligned} \Omega_L &= \{\mathbf{x} \in \mathbb{R}^d \mid \mathbf{a} \cdot \mathbf{x} < 0\}, \\ \Omega_R &= \{\mathbf{x} \in \mathbb{R}^d \mid \mathbf{a} \cdot \mathbf{x} > 0\}, \end{aligned} \quad \text{with} \quad \Gamma = \partial\Omega_L \cap \partial\Omega_R, \tag{11}$$

where $\mathbf{a}$ is a unit vector in $\mathbb{R}^d$. Given $(D_L(\omega), D_R(\omega), \alpha(\omega))$ where $D_L(\omega)$ and $D_R(\omega)$ are two $d \times d$ complex invertible matrices ($\forall \omega \in \mathbb{R} \setminus \{0\}$) and $\alpha(\omega)$ is a complex scalar function of ω, we introduce the transmission problem between the wave equations associated to the media $(A; D_L(\omega))$ and $(A; D_R(\omega))$:

$$
\begin{cases}
-\omega^2 \hat{u}_L - \nabla \cdot D_L^{-1} A D_L^{-T} \nabla \hat{u}_L = 0, & \mathbf{x} \in \Omega_L, \\[2mm]
-\omega^2 \hat{u}_R - \nabla \cdot D_R^{-1} A D_R^{-T} \nabla \hat{u}_R = 0, & \mathbf{x} \in \Omega_R, \\[2mm]
\hat{u}_L = \hat{u}_R, & \mathbf{x} \in \Gamma, \\[2mm]
D_L^{-1} A D_L^{-T} \nabla \hat{u}_L \cdot \mathbf{a} = \alpha \, D_R^{-1} A D_R^{-T} \nabla \hat{u}_R \cdot \mathbf{a}, & \mathbf{x} \in \Gamma.
\end{cases}
\tag{12}
$$

The next theorem gives conditions on $(D_L(\omega), D_R(\omega), \alpha(\omega))$ for the existence of solutions that propagate without reflections at the interface between Ω_L and Ω_R.

Theorem 1
Let $\omega \in \mathbb{R} \setminus \{0\}$, if

$$
D_L(\omega)\mathbf{b} = D_R(\omega)\mathbf{b} \quad \forall \, \mathbf{b} \in \mathbf{a}^\perp := \{\mathbf{b} \in \mathbb{R}^d \setminus \{0\} \quad | \quad \mathbf{b} \cdot \mathbf{a} = 0\}
\tag{13}
$$

and

$$
\alpha(\omega) = D_R^T(\omega) D_L^{-T}(\omega)\mathbf{a} \cdot \mathbf{a},
\tag{14}
$$

then for every $(\mathbf{k}_L, u_0) \in \mathbb{C}^d \times \mathbb{C}$ such that $F(\omega, D_L^{-T} \mathbf{k}_L) = 0$, the couple $(\hat{u}_L, \hat{u}_R) \in \mathbb{C} \times \mathbb{C}$ given by

$$
\hat{u}_L(\mathbf{x}) = u_0 e^{-\imath \mathbf{k}_L \cdot \mathbf{x}}, \quad \hat{u}_R(\mathbf{x}) = u_0 e^{-\imath \mathbf{k}_R \cdot \mathbf{x}},
$$

with

$$
\mathbf{k}_R = \beta_R \mathbf{a} + \underline{\mathbf{k}}_R, \quad \beta_R = D_L^{-1}(\omega) D_R(\omega)\mathbf{a} \cdot \mathbf{k}_L, \quad \underline{\mathbf{k}}_R = \mathbf{k}_L - (\mathbf{k}_L \cdot \mathbf{a})\mathbf{a},
$$

is a solution of the problem (12).

Existence, uniqueness or stability results in the appropriate functional space for such a general problem are difficult to obtain. This theorem does not state such results, but it can be interpreted as follows: if we consider an incident plane wave (evanescent or propagative) in Ω_L, and if the associated transmission problem (12) has a unique solution (this is the difficult part to prove), then there is no reflected wave in Ω_L and only one plane wave (evanescent or propagative) is transmitted in Ω_R as soon as the conditions (13) and (14) hold.

Proof
We construct explicitly a solution $\hat{u}_R$ of the form

$$
\hat{u}_R(\mathbf{x}) = u_0 e^{-\imath \mathbf{k}_R \cdot \mathbf{x}},
$$

for given $\mathbf{k}_L$ and u_0 (which determine $\hat{u}_L$) such that $F(\omega, D_L^{-T} \mathbf{k}_L) = 0$. For this purpose we write that

$$
\mathbf{k}_L = \beta_L \mathbf{a} + \underline{\mathbf{k}}_L \quad \text{and} \quad \mathbf{k}_R = \beta_R \mathbf{a} + \underline{\mathbf{k}}_R \quad \text{with } (\underline{\mathbf{k}}_L, \underline{\mathbf{k}}_R) \in (\mathbf{a}^\perp)^2.
$$

The first transmission condition (the continuity of the traces of $\hat{u}_L$ and $\hat{u}_R$ on $\Gamma = \mathbf{a}^\perp \cup \{0\}$) gives

$$
u_0 e^{-\imath \mathbf{k}_L \cdot \mathbf{b}} = u_0 e^{-\imath \mathbf{k}_R \cdot \mathbf{b}}, \quad \mathbf{b} \in \Gamma,
$$

and implies $\underline{\mathbf{k}}_R = \underline{\mathbf{k}}_L$. Hence, the second transmission condition simplifies like

$$
D_L^{-1} A D_L^{-T} \mathbf{k}_L \cdot \mathbf{a} = \alpha \, D_R^{-1} A D_R^{-T} \mathbf{k}_R \cdot \mathbf{a}.
$$

Therefore, it is sufficient to find $(\mathbf{k}_R, \alpha(\omega))$ such that

$$
\begin{cases}
D_L^{-T} \mathbf{k}_L = D_R^{-T} \mathbf{k}_R & (\Leftrightarrow D_R^T D_L^{-T} \mathbf{k}_L = \mathbf{k}_R), \\[2mm]
D_L^{-T} \mathbf{a} = \alpha \, D_R^{-T} \mathbf{a} & (\Leftrightarrow D_R^T D_L^{-T} \mathbf{a} = \alpha \, \mathbf{a}).
\end{cases}
\tag{15}
$$

The second equality of (15) is equivalent to

$$D_R^T D_L^{-T} \mathbf{a} \cdot \mathbf{a} = \alpha \quad \text{and} \quad D_R^T D_L^{-T} \mathbf{a} \cdot \mathbf{b} = 0, \quad \mathbf{b} \in \mathbf{a}^\perp,$$

which holds under the conditions (13) and (14). In the same way, the first equality of (15) is equivalent to

$$D_L^{-1} D_R \mathbf{a} \cdot \mathbf{k}_L = \mathbf{a} \cdot \mathbf{k}_R \quad \text{and} \quad D_L^{-1} D_R \mathbf{b} \cdot \mathbf{k}_L = \mathbf{b} \cdot \mathbf{k}_R, \quad \mathbf{b} \in \mathbf{a}^\perp.$$

Since we have $\underline{\mathbf{k}}_L = \underline{\mathbf{k}}_R$ and assuming that (13) is true, the previous equalities simplify to

$$\beta_R = D_L^{-1} D_R \mathbf{a} \cdot \mathbf{k}_L,$$

which gives a value for β_R and enable us to construct $\mathbf{k}_R$. Note that we have $D_L^{-T} \mathbf{k}_L = D_R^{-T} \mathbf{k}_R$, which immediately implies $F(\omega, D_R^{-T} \mathbf{k}_R) = 0$ and so $\hat{u}_R(\mathbf{x})$ is indeed a solution of the second equation of (12). $\qquad\square$

When $\mathbf{a} = \mathbf{e}_1$, this result is less general than those presented in [15] but it exhibits the parameter $\alpha(\omega)$, which enables us to define transmission problems with no parasitic reflections at a continuous level. This prefigures the numerical method developed in section 4.2.

2.4. Treatment of corner regions

In what follows we present a way to define perfectly matched media in corner/edge regions by using the geometrical assumptions of theorem 1 (equation (13)).

Corner regions in 2D. Let $\mathbb{R}^2$ be split into four parts Ω_φ, Ω_R, Ω_D and Ω_C (for physical, right, down and corner regions) with respect to the four unitary vectors $\mathbf{a}_{\varphi,R}$, $\mathbf{a}_{\varphi,D}$, $\mathbf{a}_{R,C}$ and $\mathbf{a}_{D,C}$ such that (see figure 2)

$$\begin{cases} \Omega_\varphi := \{\mathbf{x} \in \mathbb{R}^2 \quad | \quad \mathbf{a}_{\varphi,R} \cdot \mathbf{x} < 0 \quad \text{and} \quad \mathbf{a}_{\varphi,D} \cdot \mathbf{x} < 0\}, \\[2mm] \Omega_R := \{\mathbf{x} \in \mathbb{R}^2 \quad | \quad \mathbf{a}_{\varphi,R} \cdot \mathbf{x} > 0 \quad \text{and} \quad \mathbf{a}_{R,C} \cdot \mathbf{x} < 0\}, \\[2mm] \Omega_D := \{\mathbf{x} \in \mathbb{R}^2 \quad | \quad \mathbf{a}_{\varphi,D} \cdot \mathbf{x} > 0 \quad \text{and} \quad \mathbf{a}_{D,C} \cdot \mathbf{x} < 0\}, \\[2mm] \Omega_C := \{\mathbf{x} \in \mathbb{R}^2 \quad | \quad \mathbf{a}_{R,C} \cdot \mathbf{x} > 0 \quad \text{and} \quad \mathbf{a}_{D,C} \cdot \mathbf{x} > 0\}, \end{cases}$$

with

$$\mathbf{a}_{\varphi,R} \cdot \mathbf{a}_{R,C} = \mathbf{a}_{\varphi,D} \cdot \mathbf{a}_{D,C} = 0 \quad \text{and} \quad [\mathbf{a}_{\varphi,D}]_1 [\mathbf{a}_{\varphi,R}]_2 - [\mathbf{a}_{\varphi,D}]_2 [\mathbf{a}_{\varphi,R}]_1 > 0.$$

We introduce the matrices D_R and D_D related tot the media $(A; D_R)$ and $(A; D_D)$ occupying the
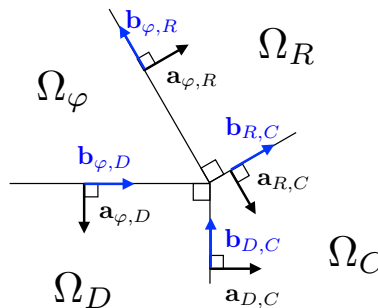

Figure 2. Corner region in 2D.

region Ω_R and Ω_D, and we assume that the perfectly matched condition condition (13) is satisfied

(dependence in ω is omitted):

$$D_R \, \mathbf{b}_{\varphi,R} \; = \; \mathbf{b}_{\varphi,R} \quad \forall \, \mathbf{b}_{\varphi,R} \, \in \, \mathbf{a}_{\varphi,R}^\perp. \quad \text{and} \quad D_D \, \mathbf{b}_{\varphi,D} \; = \; \mathbf{b}_{\varphi,D} \quad \forall \, \mathbf{b}_{\varphi,C} \, \in \, \mathbf{a}_{\varphi,C}^\perp.$$

A perfectly matched medium is built in Ω_C by introducing the matrix D_C (hence the corresponding medium $(\,A\,;\,D_C\,)$) that respects the condition (13) for the two interfaces of Ω_C:

$$D_C \, \mathbf{b}_{D,C} \; = \; D_R \, \mathbf{b}_{D,C} \quad \text{and} \quad D_C \, \mathbf{b}_{R,C} \; = \; D_D \, \mathbf{b}_{R,C}.$$

As $\mathbf{b}_{R,C}$ and $\mathbf{b}_{D,E}$ form a free basis of $\mathbb{R}^2$, these last conditions uniquely characterize D_C.

Remark 1
$D_C = D_R + D_D - I$ when $\mathbf{a}_{\varphi,R} \cdot \mathbf{a}_{\varphi,D} = 0$ (where I is the $d \times d$ identity matrix).

The previous geometrical construction arguments can be extend in a very similar way to define perfectly matched media in edge regions and corner regions in 3D.

Edge regions in 3D.   Using the same notation, we extrude the previous split plane along the third dimension ($\mathbf{b}_3$). Then, the matrices D_R and D_D (which are now 3×3 matrices) also satisfy

$$D_R \, \mathbf{b}_3 \; = \; \mathbf{b}_3 \quad \text{and} \quad D_D \, \mathbf{b}_3 \; = \; \mathbf{b}_3,$$

and the matrix D_E (we replace the index C with E for edge instead of corner) must respect the additional condition

$$D_E \, \mathbf{b}_3 \; = \; D_R \, \mathbf{b}_3 \; = \; D_D \, \mathbf{b}_3 \; = \; \mathbf{b}_3.$$

Corner regions in 3D.   We now consider three vectors $\mathbf{a}_i$ ($1 \le i \le 3$) forming a direct but non necessarily orthogonal basis of $\mathbb{R}^3$ and we define

$$\begin{cases} \Omega_{E_i} := \{ \mathbf{x} \in \mathbb{R}^3 \;\;|\;\; \mathbf{a}_i \cdot \mathbf{x} < 0 \quad \text{and} \quad \mathbf{a}_j \cdot \mathbf{x} > 0 \quad \forall \, j \ne i \}, \quad 1 \le i \le 3, \\[2mm] \Omega_C := \{ \mathbf{x} \in \mathbb{R}^3 \;\;|\;\; \mathbf{a}_i \cdot \mathbf{x} > 0, \quad 1 \le i \le 3 \}. \end{cases}$$

In each edge region Ω_{E_i}, we assume given the media $(\,A\,;\,D_{E_i}\,)$ that satisfies the previous perfectly matched conditions. Hence the suitable matrix D_C, defining the medium $(\,A\,;\,D_C\,)$ in the corner region Ω_C, is the unique matrix that respects

$$D_C \, \mathbf{b}_i \; = \; D_{E_i} \, \mathbf{b}_i \quad \forall \, \mathbf{b}_i \in \mathbf{a}_i^\perp, \quad 1 \le i \le 3.$$

2.5. Stability of the PML in time domain

We now consider that $\mathbf{k}$ is a given real wavenumber, and ω is the solution of the modified dispersion relation (10) which is not necessarily real anymore. Exponential decreasing or growing behavior in time domain can occur depending on the sign of its imaginary part. This leads to the definition of an absorbing or unstable medium.

Definition 2
Let $\omega(\mathbf{k})$ be the solution of the modified dispersion relation (10). A medium characterized by $(\,A\,;\,D(\omega)\,)$ (8) is said to be

- stable[†] if $\Im m\big(\omega(\mathbf{k})\big) \ge 0 \; \forall \, \mathbf{k} \in \mathbb{R}^d$ (unstable if $\exists \mathbf{k}$ such that $\Im m\big(\omega(\mathbf{k})\big) < 0$),
- an absorbing medium if it is stable and if $\Im m\big(\omega(\mathbf{k})\big) > 0$ for almost every $\mathbf{k}$.

[†]A rigorous framework is needed to prove that absorbing media provide stable and/or decreasing solutions in time domain. We refer to [8, 16] for presentations of this theoretical framework.

We now assume a specific dependence in ω for the matrices $D(\omega)$. More precisely, we focus on media $(A_{ij} \, ; \, D(\omega))$ obtained by the change of variables which is commonly used in the literature [5] to define absorbing media. We choose

$$D(\omega) := D_1 - \frac{\imath}{\omega} D_2, \tag{16}$$

where D_1 and D_2 are $d \times d$ real matrices, D_1 being invertible.

Definition 3
As an alternative to definition 1, when the change of variable is of the form (16), the corresponding complex medium can be defined by the set of three $d \times d$ real matrices denoted by $\big(A \, ; \, (D_1, D_2) \big)$.

This new definition is related to definition 1 by the relation

$$\big(A \, ; \, (D_1, D_2) \big) \equiv \big(A \, ; \, D_1 - \frac{\imath}{\omega} D_2 \big).$$

Referring to the previous section, we see that this change of variable is perfectly matched with the physical medium $(A \, ; \, I)$ (*i.e.* it respects condition (13) with $D_L = I$ and $D_R = D(\omega)$) for the direction $\mathbf{a}$ when

$$D_1 \mathbf{b} = \mathbf{b} \text{ and } D_2 \mathbf{b} = 0, \quad \forall \mathbf{b} \in \mathbf{a}^\perp. \tag{17}$$

The following theorem gives a necessary condition to obtain a stable medium characterized by $\big(A \, ; \, (D_1, D_2) \big)$. It generalizes the theorem stated in [8] which is based upon a high frequency analysis (*i.e.* $|\mathbf{k}|^{-1}$ is considered as a small parameter).

Theorem 2
(**High Frequency Stability - HFS**) A stable medium $\big(A \, ; \, (D_1, D_2) \big)$ has to verify

$$D_1^{-1} D_2 D_1^{-1} A \mathbf{K} \cdot \mathbf{K} \geq 0,$$

for all vector $\mathbf{K} \in \mathbb{S}^d$.

Proof
We have to prove that for sufficiently small $\varepsilon = |\mathbf{k}|^{-1}$ we have

$$\Im \mathrm{m}(\mathcal{V}) \geq 0 \quad \forall \mathcal{V} \text{ satisfying } \tilde{F}(\mathcal{V}, \mathbf{K}) = F(\mathcal{V}, [D_1 - \frac{\imath \varepsilon}{\mathcal{V}} D_2]^{-T} \mathbf{K}) = 0.$$

To this end, an asymptotic development of $\mathcal{V}$ in power of ε of the form

$$\mathcal{V} = \mathcal{V}_0 + \varepsilon \mathcal{V}_1 + O(\varepsilon^2) \quad \text{with} \quad F(\mathcal{V}_0, D_1^{-T} \mathbf{K}) = 0 \tag{18}$$

is substituted in the modified dispersion relation :

$$F(\mathcal{V}_0 + \varepsilon \mathcal{V}_1 + O(\varepsilon^2), [D_1 - \frac{\imath \varepsilon}{\mathcal{V}_0 + \varepsilon \mathcal{V}_1 + O(\varepsilon^2)} D_2]^{-T} \mathbf{K}) = 0.$$

Then, the implicit function theorem is used around $\varepsilon = 0$ to obtain

$$F(\mathcal{V}_0, D_1^{-T} \mathbf{K}) + \varepsilon \big[\mathcal{V}_1 \frac{\partial}{\partial \omega} F(\mathcal{V}_0, D_1^{-T} \mathbf{K}) + \gamma \cdot \nabla_{\mathbf{k}} F(\mathcal{V}_0, D_1^{-T} \mathbf{K}) \big] + O(\varepsilon^2) = 0 \tag{19}$$

with

$$\gamma = \Big(\frac{d}{d\varepsilon} [D_1 - \frac{\imath \varepsilon}{\mathcal{V}_0 + \varepsilon \mathcal{V}_1 + O(\varepsilon^2)} D_2]^{-T} \mathbf{K} \Big)_{|\varepsilon=0} = +\frac{\imath}{\mathcal{V}_0} [D_1^{-1} D_2 D_1^{-1}]^T \mathbf{K}.$$

By definition of $\mathcal{V}_0$ the term $F(\mathcal{V}_0, D_1^{-T} \mathbf{K})$ in (19) vanishes and after identification of the ε powers we see that we must have

$$\mathcal{V}_1 \frac{\partial}{\partial \omega} F(\mathcal{V}_0, D_1^{-T} \mathbf{K}) + \gamma \cdot \nabla_{\mathbf{k}} F(\mathcal{V}_0, D_1^{-T} \mathbf{K}) = 0$$

which implies that

$$
\begin{aligned}
\mathcal{V}_1 &= -\imath\big(\frac{\partial}{\partial\omega}F(\mathcal{V}_0, D_1^{-T}\mathbf{K})\big)^{-1}[D_1^{-1}D_2D_1^{-1}]^T\frac{\mathbf{K}}{\mathcal{V}_0}\cdot\nabla_{\mathbf{k}}F(\mathcal{V}_0, D_1^{-T}\mathbf{K}) \\
&= \imath D_1^{-1}D_2D_1^{-1}V(\mathbf{K})\cdot S(\mathbf{K}) = \imath\, a(\mathbf{k})^{-1}\, D_1^{-1}D_2D_1^{-1}A\mathbf{K}\cdot\mathbf{K}.
\end{aligned}
$$

We see in equation (18) that the sign of the imaginary part of $\mathcal{V}$ is given by by the sign of the imaginary part of $\mathcal{V}_1$ choosing ε small enough (since $\mathcal{V}_0$ is real).

$\square$

Using basic algebraic arguments one can prove the following lemma which will be useful in order to simplify the HFS analysis.

Lemma 1
The stability condition stated in theorem 2 is satisfied for this medium $\big(A\,;(D_1, D_2)\big)$ if and only if it is satisfied for the medium $\big(\tilde{A}\,;(I, \tilde{D}_2)\big)$ with

$$
\tilde{A} = D_1^{-1}AD_1^{-T} \quad\text{and}\quad \tilde{D}_2 = D_1^{-1}D_2.
$$

Although it is only a sufficient condition, the HFS condition is the cornerstone of the stability analysis addressed in the following of the paper. Note that instability phenomena can be observed at intermediate frequencies (see [17, 2] for instance in elastodynamics). One solution to avoid these instabilities is to use the so called complex frequency shift technique for which (16) is replaced by

$$
D(\omega) := D_1 - \frac{\imath}{\omega - \imath\gamma}D_2, \quad \gamma \in \mathbb{R}.
$$

3. CONSTRUCTION OF PML FOR ANISOTROPIC MEDIA

In the following, τ will refer to the damping function and will be a positive constant. In practice we actually use a constant damping function but the following analysis can be extended to varying damping functions using the theory developed in [16].

3.1. *The half-space problem with the classical change of variable*

We consider the transmission problem (12) for a given unitary vector $\mathbf{a}$. We point out the fact that the classical PML change of variable leading to the medium $\big(A\,;(D_1, D_2)\big)$, with D_1 and D_2 defined by (16) with

$$
D_1 = I \quad\text{and}\quad D_2 = \tau\,\mathbf{a}\,\mathbf{a}^T \tag{20}
$$

may generate an unstable medium (although satisfying the perfectly matched transmission conditions of theorem 1).

Corollary 1
Assume $\tau \neq 0$, the medium obtained using (20) satisfies the HFS condition of theorem 2 if and only if $\tau > 0$ and $A\,\mathbf{a}\cdot\mathbf{b} = 0$ for all $\mathbf{b}\in\mathbf{a}^\perp$.

Proof
We have $D_1^{-1}D_2D_1^{-1} = \tau\,\mathbf{a}\,\mathbf{a}^T$, so we need to check that

$$
\mathbf{a}\,\mathbf{a}^T A\mathbf{K}\cdot\mathbf{K} \geq 0 \quad \forall\,\mathbf{K}\in\mathbb{S}^d \quad\Leftrightarrow\quad (A\mathbf{K}\cdot\mathbf{a})(\mathbf{K}\cdot\mathbf{a}) \geq 0 \quad \forall\,\mathbf{K}\in\mathbb{S}^d.
$$

Now assume that $\mathbf{K} = \alpha_{\mathbf{K}}\,\mathbf{a} + \mathbf{b}_{\mathbf{K}}$ with $\alpha_{\mathbf{K}}$ a real scalar and $\mathbf{b}_{\mathbf{K}}\in\mathbf{a}^\perp$, we find

$$
(A\mathbf{K}\cdot\mathbf{a})(\mathbf{K}\cdot\mathbf{a}) = \alpha_{\mathbf{K}}(A\mathbf{a}\cdot\mathbf{a}) + (A\mathbf{b}_{\mathbf{K}}\cdot\mathbf{a})
$$

by letting $\alpha_{\mathbf{K}}$ tends to 0, we see that the previous quantity is positive for all $\mathbf{K}\in\mathbb{S}^d$ if and only if $A\mathbf{b}_{\mathbf{K}}\cdot\mathbf{a}$ is positive. As $\mathbf{b}_{\mathbf{K}}$ has been chosen arbitrarily in $\mathbf{a}^\perp$, this is true only if $A\mathbf{b}\cdot\mathbf{a} = 0$ for all $\mathbf{b}\in\mathbf{a}^\perp$.

$\square$

The previous demonstration shows that high frequency instabilities occur with grazing waves, *i.e.* plane waves that propagate with an incidence nearly parallel to the interface between the physical and absorbing domains (i.e. $\alpha_{\mathbf{K}} \simeq 0$).

3.2. *The half-space problem with an improved change of variable*

Consider again the transmission problem (12) with a given unitary vector $\mathbf{a}$. We introduce some real parameters θ_m and γ_m, $2 \leq m \leq d$, in the matrices D_1 and D_2 (resp.) like

$$D_1 = I + \sum_{m=2}^{d} \theta_m \mathbf{b}_m \mathbf{a}^T \quad \text{and} \quad D_2 = \tau \left(\mathbf{a}\,\mathbf{a}^T + \sum_{m=2}^{d} \gamma_m \mathbf{b}_m \mathbf{a}^T \right), \tag{21}$$

with

$$\text{span}\{\,\mathbf{b}_m,\ 2 \geq m \geq d\,\} = \mathbf{a}^\perp, \quad |\mathbf{b}_m| = 1, \quad 2 \geq m \geq d,$$

and study their effect on the stability condition. Note that D_1 and D_2 respect the perfectly matched condition (17). Using lemma 1 we are able to define appropriate parameters θ_m and γ_m such that the HFS condition is satisfied for any matrix A satisfying assumption 1.

Theorem 3
The medium $\big(A\,;\,(D_1, D_2) \big)$ defined by (21) with

$$\tau > 0 \quad \text{and} \quad \theta_m = \gamma_m = \frac{A\mathbf{a} \cdot \mathbf{b}_m}{A\mathbf{a} \cdot \mathbf{a}}, \quad 2 \leq m \leq d,$$

respects the HFS condition stated in theorem 2.

Proof
By lemma 1 we can study the equivalent medium $\big(\tilde{A}\,;\,(I, \tilde{D}_2) \big)$ with

$$\tilde{A} = D_1^{-1} A D_1^{-T} = A - \sum_{m=2}^{d} \theta_m [\mathbf{b}_m \mathbf{a}^T A + A\,\mathbf{a}\mathbf{b}_m^T] + (A\mathbf{a} \cdot \mathbf{a}) \sum_{m,n=2}^{d} \theta_m \theta_n \mathbf{b}_m \mathbf{b}_n^T,$$

$$\tilde{D}_2 = D_1^{-1} D_2 = \tau\,\mathbf{a}\,\mathbf{a}^T + \tau \sum_{m=2}^{d} \gamma_m \mathbf{b}_m \mathbf{a}^T - \tau \sum_{m=2}^{d} \theta_m \mathbf{b}_m \mathbf{a}^T,$$

then we can check that the medium $\big(\tilde{A}\,;\,(I, \tilde{D}_2) \big)$ satisfies the necessary condition stated in corollary 1 when $\theta_m = \gamma_m = A\mathbf{a} \cdot \mathbf{b}_m / A\mathbf{a} \cdot \mathbf{a}$. $\qquad\square$

Remark 2
We obtain the relation

$$D(\omega) = D_1 - \frac{\imath}{\omega} D_2 = D_1 (I - \tau \frac{\imath}{\omega} \mathbf{a}\mathbf{a}^T), \tag{22}$$

which can be interpreted as follows. First, the propagative medium is changed (in a perfectly matched way) from A to $\tilde{A} = D_1^{-1} A D_1^{-T}$ and, second, some absorption (again in a perfectly matched manner) is added in the direction $\mathbf{a}$. It leads to a stable medium since corollary 1 is now satisfied.

Finally, as it will be used later to define the numerical scheme, we consider the transmission problem (12) between the physical domain Ω_L ($D_L := I$) and the perfectly matched layer Ω_R ($D_R := D_1 - (\imath/\omega)D_2$). The transmission parameter $\alpha(\omega)$ is given by

$$\alpha(\omega) = D_R^T(\omega)\,D_L^{-T}(\omega)\,\mathbf{a} \cdot \mathbf{a} = \frac{\omega - \imath\tau}{\omega} \tag{23}$$

while the transmission condition

$$D_L^{-1}(\omega) A D_L^{-T}(\omega) \nabla \hat{u}_L \cdot \mathbf{a} = \alpha(\omega) D_R^{-1}(\omega) A D_R^{-T}(\omega) \nabla \hat{u}_R \cdot \mathbf{a}$$

is written as

$$
\begin{aligned}
A\nabla\hat{u}_L \cdot \mathbf{a} &= \alpha(\omega)(I - \tau\frac{\imath}{\omega}\mathbf{a}\mathbf{a}^T)^{-1}\tilde{A}_R(I - \tau\frac{\imath}{\omega}\mathbf{a}\,\mathbf{a}^T)^{-T}\nabla\hat{u}_R \cdot \mathbf{a}, \\
&= \frac{\omega - \imath\tau}{\omega}\,(I + \frac{\imath\,\tau}{\omega - \imath\,\tau}\mathbf{a}\,\mathbf{a}^T)\tilde{A}_R(I - \tau\frac{\imath}{\omega}\mathbf{a}\,\mathbf{a}^T)^{-T}\nabla\hat{u}_R \cdot \mathbf{a},
\end{aligned}
$$

and simplifies like

$$
A\nabla\hat{u}_L \cdot \mathbf{a} = \tilde{A}_R(I - \tau\frac{\imath}{\omega}\mathbf{a}\,\mathbf{a}^T)^{-T}\nabla\hat{u}_R \cdot \mathbf{a}. \tag{24}
$$

3.3. *The corner region in 2D polygonal domains.*

The tools developed in section 2 allow us to handle PML in any corner of a polygonal convex domain. Here we prove the high frequency stability condition for the new media defined in the corner region that is depicted in section 2.4 (see figure 2). According to definition 3, we refer to the triplets $\big(A\,;(D_{R,1},D_{R,2})\big)$, $\big(A\,;(D_{D,1},D_{D,2})\big)$ and $\big(A\,;(D_{C,1},D_{C,2})\big)$ to define the absorbing media in Ω_R, Ω_D and Ω_C respectively. $D_{R,1}, D_{R,2}, D_{D,1}, D_{D,2}$ are obtained using the result of the half-space study presented below:

$$
D_{R,1} = I + \theta_R\,\mathbf{a}_{R,C}\mathbf{a}_{\varphi,R}^T \qquad D_{R,2} = \tau\,\mathbf{a}_{\varphi,R}\mathbf{a}_{\varphi,R}^T + \tau\,\theta_R\,\mathbf{a}_{R,C}\mathbf{a}_{\varphi,R}^T,
$$

$$
D_{D,1} = I + \theta_D\,\mathbf{a}_{D,C}\mathbf{a}_{\varphi,D}^T \qquad D_{D,2} = \tau\,\mathbf{a}_{\varphi,D}\mathbf{a}_{\varphi,D}^T + \tau\,\theta_R\,\mathbf{a}_{D,C}\mathbf{a}_{\varphi,D}^T,
$$

with

$$
\theta_R = \frac{A\mathbf{a}_{\varphi,R} \cdot \mathbf{a}_{R,C}}{A\mathbf{a}_{\varphi,R} \cdot \mathbf{a}_{\varphi,R}} \quad \text{and} \quad \theta_D = \frac{A\mathbf{a}_{\varphi,D} \cdot \mathbf{a}_{D,C}}{A\mathbf{a}_{\varphi,D} \cdot \mathbf{a}_{\varphi,D}}. \tag{25}
$$

Hence, $(D_{C,1}, D_{C,2})$ must satisfy the constraints

$$
\begin{aligned}
\big(D_{C,1} - \frac{\imath}{\omega}D_{C,2}\big)\mathbf{a}_{\varphi,D} &= \big(D_{D,1} - \frac{\imath}{\omega}D_{D,2}\big)\mathbf{a}_{\varphi,D} = D_{D,1}\big(I - \tau\frac{\imath}{\omega}\mathbf{a}_{\varphi,D}\mathbf{a}_{\varphi,D}^T\big)\mathbf{a}_{\varphi,D}, \\
\big(D_{C,1} - \frac{\imath}{\omega}D_{C,2}\big)\mathbf{a}_{\varphi,R} &= \big(D_{R,1} - \frac{\imath}{\omega}D_{R,2}\big)\mathbf{a}_{\varphi,R} = D_{R,1}\big(I - \tau\frac{\imath}{\omega}\mathbf{a}_{\varphi,R}\mathbf{a}_{\varphi,R}^T\big)\mathbf{a}_{\varphi,R}.
\end{aligned}
$$

This suggests that we seek $(D_{C,1}, D_{C,2})$ under the form

$$
D_{C,1} - \frac{\imath}{\omega}D_{C,2} = (1 - \tau\frac{\imath}{\omega})D_{C,1} \quad \Rightarrow \quad D_{C,2} = \tau D_{C,1} \tag{26}
$$

where $D_{C,1}$ is uniquely defined by the two linear constraints

$$
D_{C,1}\mathbf{a}_{\varphi,D} = D_{D,1}\mathbf{a}_{\varphi,D}, \quad D_{C,1}\mathbf{a}_{\varphi,R} = D_{R,1}\mathbf{a}_{\varphi,R}. \tag{27}
$$

The matrix $D_{C,1}$ is invertible thanks to the following result

Lemma 2
Vectors $D_{R,1}\mathbf{a}_{\varphi,R}$ and $D_{D,1}\,\mathbf{a}_{\varphi,D}$ are independent.

Proof
We just give a sketch of the proof. First we can remark that, by construction,

$$
D_{R,1}\mathbf{a}_{\varphi,R} = \mathbf{a}_{\varphi,R} + \theta_R\mathbf{a}_{R,C} \quad \text{and} \quad D_{D,1}\,\mathbf{a}_{\varphi,D} = \mathbf{a}_{\varphi,D} + \theta_D\mathbf{a}_{D,C}.
$$

Then, taking into account the definition of θ_R and θ_D (25), we need to prove that

$$
(A\mathbf{a}_{\varphi,R} \cdot \mathbf{a}_{\varphi,R})\mathbf{a}_{\varphi,R} + (A\mathbf{a}_{\varphi,R} \cdot \mathbf{a}_{R,C})\mathbf{a}_{R,C} \quad \text{and} \quad (A\mathbf{a}_{\varphi,D} \cdot \mathbf{a}_{\varphi,D})\mathbf{a}_{\varphi,D} + (A\mathbf{a}_{\varphi,D} \cdot \mathbf{a}_{D,C})\mathbf{a}_{D,C}
$$

are independent. Now, defining (λ_1, λ_2) the eigenvalues of A associated to the unitary eigenvectors $(\mathbf{q}_1, \mathbf{q}_2)$ then algebraic manipulations show that for $P \equiv R$ or $P \equiv D$ the previous relations can be simplified as follows,

$$\mathbf{a}_{\varphi,P} = \alpha_{P,1}\mathbf{q}_1 + \alpha_{P,2}\mathbf{q}_2 \Rightarrow (A\mathbf{a}_{\varphi,P} \cdot \mathbf{a}_{\varphi,P})\mathbf{a}_{\varphi,P} + (A\mathbf{a}_{\varphi,P} \cdot \mathbf{a}_{P,C})\mathbf{a}_{P,C} = \alpha_{P,1}\lambda_1\mathbf{q}_1 + \alpha_{P,2}\lambda_2\mathbf{q}_2.$$

This implies that $D_{R,1}\mathbf{a}_{\varphi,R}$ and $D_{D,1}\mathbf{a}_{\varphi,D}$ are not independent only if $\mathbf{a}_{\varphi,R}$ and $\mathbf{a}_{\varphi,D}$ are not independent, which is impossible by construction.

<div style="text-align: right">□</div>

We can now state the main result concerning the PML in the corner region:

Theorem 4
The media $(A,\ D_{C,1},\ D_{C,2})$ defined by (26) and (27) satisfies the HFS condition.

Proof
Since $D_{C,1}^{-1}D_{C,2} = \tau I$, we need to check, from lemma 1, the high frequency stability condition for the equivalent medium $(D_{C,1}^{-1}AD_{C,1}^{-T},\ I,\ I)$, which is trivially satisfied.

<div style="text-align: right">□</div>

To define properly our problem at the continuous and discrete levels we need to specify the transmission conditions at the interface of the absorbing layers. In what follows, the real parameter α_{RC} (α_{DC} resp.) is used in the transmission equation (12) of the flux between Ω_R and Ω_C (between Ω_D and Ω_C resp.). Following theorem 1 we have

$$\begin{aligned}
\alpha_{RC} &= (D_{C,1} - \frac{\iota}{\omega}D_{C,2})^T(D_{R,1} - \frac{\iota}{\omega}D_{R,2})^{-T}\mathbf{a}_{R,C} \cdot \mathbf{a}_{R,C} \\
&= (1 - \tau\frac{\iota}{\omega})D_{C,1}^T D_{R,1}^{-T}\big(I - \tau\frac{\iota}{\omega}\mathbf{a}_{\varphi,R}\mathbf{a}_{\varphi,R}^T\big)^{-T}\mathbf{a}_{R,C} \cdot \mathbf{a}_{R,C} \\
&= D_{C,1}^T D_{R,1}^{-T}\mathbf{a}_{R,C} \cdot \mathbf{a}_{R,C}
\end{aligned}$$

and, with the same algebraic manipulations (note that the algebraic relation (30) introduced later has been used)

$$\alpha_{DC} = D_{C,1}^T D_{D,1}^{-T}\mathbf{a}_{D,C} \cdot \mathbf{a}_{D,C}$$

3.4. The corner regions in 2D in a rectangular domain.

Here we consider the specific (but commonly used) case for which $\mathbf{a}_R = \mathbf{e}_1$ and $\mathbf{a}_D = \mathbf{e}_2$. The matrices $D_{R,1}, D_{R,2}, D_{D,1}, D_{D,2}$ are given by

$$D_{R,1} = \begin{bmatrix} 1 & 0 \\ [A]_{12}/[A]_{11} & 1 \end{bmatrix}, \qquad D_{R,2} = \begin{bmatrix} \tau & 0 \\ [A]_{12}/[A]_{11} & 0 \end{bmatrix},$$

$$D_{D,1} = \begin{bmatrix} 1 & [A]_{12}/[A]_{22} \\ 0 & 1 \end{bmatrix}, \qquad D_{D,2} = \begin{bmatrix} 0 & [A]_{12}/[A]_{22} \\ 0 & \tau \end{bmatrix},$$

while $D_{E,1} = D_{R,1} + D_{D,1} - I$ and $D_{E,2} = D_{R,2} + D_{D,2}$. As explained before the equivalent medium $\big(\tilde{A};\ (I,\tilde{D}_2)\big)$ is well defined (i.e $D_{E,1}$ is invertible). More precisely we have

$$\begin{aligned}
\tilde{A} &= [D_{C,1}]^{-1}\,A\,[D_{C,1}]^{-T} = \frac{[A]_{11}[A]_{22}}{[A]_{11}[A]_{22} - [A]_{12}^2}\begin{bmatrix} [A]_{11} & -[A]_{12} \\ -[A]_{12} & [A]_{22} \end{bmatrix}, \\
\tilde{D}_2 &= [D_{C,1}]^{-1}D_{C,2} = \tau I.
\end{aligned} \qquad (28)$$

The parameters α_{RC} and α_{DC} required to define the transmission problems are given by (14) and read

$$\alpha_{RC} = \alpha_{DC} = \frac{[A]_{11}[A]_{22} - [A]_{12}^2}{[A]_{11}[A]_{22}}.$$

Explicit discretization of the anisotropic equation (3) leads to a stable scheme under a condition on the time step of the form

$$\Delta t \le C(\Omega_h, p)\frac{h}{c_{max}},$$

where $C(\Omega_h, p)$ is a constant that depends on both the shape of the mesh Ω_h and the order p of the finite element method, h is the mesh size and c_{max} is the spectral radius of the matrix A. In corner regions, the propagation of the wave is done in the medium $\left(\tilde{A} \, ; (I, \tilde{D}_2) \right)$ with $\tilde{A}$ defined by (28), which leads to the more severe time step restriction

$$\Delta t \leq C(\Omega_h, p) \frac{[A]_{11}[A]_{22} - [A]_{12}^2}{[A]_{11}[A]_{22}} \frac{h}{c_{max}}.$$

We recall that assumption 1 implies that $([A]_{11}[A]_{22} - [A]_{12}^2)$ is strictly positive. Note that the domain decomposition technique introduced in the next section may yield more naturally to the use of a local time step or of an implicit computation in corners in order to overcome this penalization.

Remark 3
The extension to 3D of the construction procedure and of stability results is rather straightforward in rectangular domain.

4. PRACTICAL IMPLEMENTATION OF THE PML IN TIME DOMAIN

A natural question that arises for transient simulation is how to formulate problem (7) with the complex medium defined by (8,16) to obtain a suitable time dependent variational formulation. We present a variant of the split formulation inspired by the one introduced in [1] for Maxwell equations and in [6] for elastodynamic equations which is adapted to anisotropic media in polygonal domains. This formulation and the associated transmission problem are presented in section 4.1. Mortar elements are introduced in section 4.2 to handle the corresponding weak formulation and the corresponding discretization scheme is developed. At this stage we restrict the presentation to the treatment of the transmission problem given by (12).

4.1. The split equations for the transmission problem

We consider the specific matrix (22), which results from the analysis done in section 3.2,

$$D(w) := D_1 \left(I - \tau \frac{\iota}{\omega} \mathbf{a}\,\mathbf{a}^T \right),$$

where D_1 is a constant $d \times d$ real and invertible matrix explicitly given by theorem 3 . The first step is to write the corresponding second order problem (7) (we recall that $\tilde{A} = D_1^{-T} A D_1^{-1}$),

$$-\omega^2 \hat{u} - \nabla \cdot \left(I - \tau \frac{\iota}{\omega} \mathbf{a}\,\mathbf{a}^T \right)^{-1} \tilde{A} \left(I - \tau \frac{\iota}{\omega} \mathbf{a}\,\mathbf{a}^T \right)^{-1} \nabla \hat{u} = 0, \qquad (29)$$

as a first order problem by introducing an auxiliary vector variable $\hat{v}$,

$$\begin{cases} \iota\omega \hat{u} - \nabla \cdot \left(I - \tau \frac{\iota}{\omega} \mathbf{a}\,\mathbf{a}^T \right)^{-1} \tilde{A}\hat{v} = 0, \\[2mm] \iota\omega \hat{v} - \left(I - \tau \frac{\iota}{\omega} \mathbf{a}\,\mathbf{a}^T \right)^{-1} \nabla \hat{u} = 0. \end{cases}$$

Next, using the decomposition $I = I - \mathbf{a}\,\mathbf{a}^T + \mathbf{a}\,\mathbf{a}^T$ and the equalities

$$\left(I - \tau \frac{\iota}{\omega} \mathbf{a}\,\mathbf{a}^T \right)^{-1} (I - \mathbf{a}\,\mathbf{a}^T) = I - \mathbf{a}\,\mathbf{a}^T, \qquad \left(I - \tau \frac{\iota}{\omega} \mathbf{a}\,\mathbf{a}^T \right)^{-1} \mathbf{a}\,\mathbf{a}^T = \frac{\omega}{\omega - i\tau} \mathbf{a}\,\mathbf{a}^T, \qquad (30)$$

the first order system is split like

$$\begin{cases} \iota\omega \hat{u}_0 - \nabla \cdot \left((I - \mathbf{a}\,\mathbf{a}^T)\tilde{A}\hat{v} \right) = 0, \\[2mm] \iota\omega \hat{u}_\tau - \frac{\omega}{\omega - i\tau} \nabla \cdot \left(\mathbf{a}\,\mathbf{a}^T \tilde{A}\hat{v} \right) = 0, \\[2mm] \iota\omega \hat{v} - \left(I - \tau \frac{\iota}{\omega} \mathbf{a}\,\mathbf{a}^T \right)^{-1} \nabla(\hat{u}_0 + \hat{u}_\tau) = 0. \end{cases} \qquad (31)$$

Notice that the splitting is performed on $\hat{u}$ only, which is obtained by setting $\hat{u} = \hat{u}_0 + \hat{u}_\tau$. Further simplifications and an inverse Fourier transform lead to the time domain problem

$$
\begin{cases}
\dfrac{\partial}{\partial t} u_0 - \nabla \cdot \left((I - \mathbf{a}\,\mathbf{a}^T)\tilde{A}v \right) = 0, \\[2ex]
\dfrac{\partial}{\partial t} u_\tau - \nabla \cdot \left(\mathbf{a}\,\mathbf{a}^T \tilde{A}v \right) + \tau\, u_\tau = 0, \\[2ex]
\dfrac{\partial}{\partial t} v - \nabla(u_0 + u_\tau) + \tau \mathbf{a}\,\mathbf{a}^T v = 0.
\end{cases}
\tag{32}
$$

Remark 4

The plane waves which are solutions of the problem (29) are solutions of the problem (31) but the converse is not true. Indeed, the split formulation introduce $(d-1)$ additional solutions that we need to characterize to study completely the stability of the split problem (see for instance [17]).

Now, let $\hat{u}_L$ and $\hat{u}_R$ be the solutions of the transmission problem (12) for the half space problem with

$$
D_L := I \quad D_R := D_1(I - \tau \frac{\imath}{\omega} \mathbf{a}\,\mathbf{a}^T).
$$

The transmission parameter $\alpha(\omega)$ is given by (23) while the second transmission condition (24) is equivalent to (by definition of the corresponding auxiliary variable $\hat{v}_R$)

$$
A\nabla u_L \cdot \mathbf{a} = \tilde{A}_R \frac{\partial}{\partial t} v_R \cdot \mathbf{a}.
$$

The split time dependent transmission problem is then given by

$$
\begin{cases}
\dfrac{\partial^2}{\partial t^2} u_L - \nabla \cdot A\nabla u_L = 0, & (\Omega_L), \\[2ex]
\dfrac{\partial}{\partial t} u_{R,0} - \nabla \cdot \left((I - \mathbf{a}\,\mathbf{a}^T)\tilde{A}_R v_R \right) = 0, & (\Omega_R), \\[2ex]
\dfrac{\partial}{\partial t} u_{R,\tau} - \nabla \cdot \left(\mathbf{a}\,\mathbf{a}^T \tilde{A}_R v_R \right) + \tau\, u_{R,\tau} = 0, & (\Omega_R), \\[2ex]
\dfrac{\partial}{\partial t} v_R - \nabla(u_{R,0} + u_{R,\tau}) + \tau \mathbf{a}\,\mathbf{a}^T v_R = 0, & (\Omega_R), \\[2ex]
u_L - u_{R,0} - u_{R,\tau} = 0, & (\Gamma), \\[2ex]
A\nabla u_L \cdot \mathbf{a} - \tilde{A}_R \dfrac{\partial}{\partial t} v_R \cdot \mathbf{a} = 0, & (\Gamma).
\end{cases}
\tag{33}
$$

The variational formulation of (33) can be handled by using Lagrange multipliers when treating the transmission conditions explicitly.

4.2. Non-overlapped mortar elements for perfectly matched layers

We introduce the Lagrangian multiplier λ associated to the fluxes through Γ as

$$
\lambda = \tilde{A}v_R \cdot \mathbf{a} \quad \text{and} \quad A\nabla u_L \cdot \mathbf{a} = \frac{\partial}{\partial t}\lambda.
\tag{34}
$$

Introducing the variational spaces

$$
\mathcal{U}_L = H^1(\Omega_L), \ \ \mathcal{U}_R = H^1(\Omega_R), \ \ \mathcal{V}_R = \left(L^2(\Omega_R) \right)^d \ \text{ and } \ \mathcal{L} = H^{-1/2}(\Gamma),
$$

the variational form of the coupling (33) is

$$
\begin{cases}
\text{Find } u_L(t), u_{R,0}(t), u_{R,\tau}(t), v_R(t), \lambda(t) : \mathbb{R}^+ \to \mathcal{U}_L \times \mathcal{U}_R{}^2 \times \mathcal{V}_R \times \mathcal{L} \text{ such that} \\[2mm]
\dfrac{\partial^2}{\partial t^2} \displaystyle\int_{\Omega_L} u_L \tilde{u}_L \, d\mathbf{x} + \int_{\Omega_L} A\nabla u_L \cdot \nabla \tilde{u}_L \, d\mathbf{x} - \dfrac{\partial}{\partial t} \int_{\Gamma} \lambda \tilde{u}_L \, d\mathbf{x} = 0, \\[4mm]
\dfrac{\partial}{\partial t} \displaystyle\int_{\Omega_R} u_{R,0} \tilde{u}_R \, d\mathbf{x} + \int_{\Omega_R} (I - \mathbf{a}\mathbf{a}^T) \tilde{A}_R v_R \cdot \nabla \tilde{u}_R \, d\mathbf{x} = 0, \\[4mm]
\dfrac{\partial}{\partial t} \displaystyle\int_{\Omega_R} u_{R,\tau} \tilde{u}_R \, d\mathbf{x} + \int_{\Omega_R} \mathbf{a}\mathbf{a}^T \tilde{A}_R v_R \cdot \nabla \tilde{u}_R \, d\mathbf{x} + \int_{\Gamma} \lambda \tilde{u}_R \, d\mathbf{x} + \tau \int_{\Omega_R} u_{R,\tau} \tilde{u}_R \, d\mathbf{x} = 0, \\[4mm]
\dfrac{\partial}{\partial t} \displaystyle\int_{\Omega_R} v_R \cdot \tilde{v}_R \, d\mathbf{x} - \int_{\Omega_R} \nabla(u_{R,0} + u_{R,\tau}) \cdot \tilde{v}_R \, d\mathbf{x} + \tau \int_{\Omega_R} \mathbf{a}\mathbf{a}^T v_R \cdot \tilde{v}_R \, d\mathbf{x} = 0, \\[4mm]
\displaystyle\int_{\Gamma} u_L \tilde{\lambda} \, d\mathbf{x} - \int_{\Gamma} (u_{R,0} + u_{R,\tau}) \tilde{\lambda} \, d\mathbf{x} = 0, \\[4mm]
\text{for all } \tilde{u}_L, \tilde{u}_R, \tilde{v}_R, \tilde{\lambda} \text{ in } \mathcal{U}_L \times \mathcal{U}_R \times \mathcal{V}_R \times \mathcal{L}.
\end{cases}
\tag{35}
$$

We introduce the finite-dimensional approximation spaces

$$
\mathcal{U}_{L,h} = \text{span}\left(\{\Phi_j^L\}_{j=1}^{N_L}\right) \subset \mathcal{U}_L, \quad \mathcal{U}_{R,h} = \text{span}\left(\{\Phi_j^R\}_{j=1}^{N_R}\right) \subset \mathcal{U}_R,
$$

$$
\mathcal{V}_{R,h} = \text{span}\left(\{\Psi_j\}_{j=1}^{M}\right) \subset \mathcal{V}_R, \quad \mathcal{L}_h = \text{span}\left(\{\phi_j\}_{j=1}^{n}\right) \subset \mathcal{L}.
$$

U_L, $U_{R,0}$, $U_{R,\tau}$, V_R and Λ are the vectors associated to the decomposition of the semi-discrete unknowns in their corresponding bases. The semi-discrete algebraic version of problem (35) is

$$
\begin{cases}
[M_L] \dfrac{\partial^2}{\partial t^2} U_L + [K]U_L - [P_L]^T \dfrac{\partial}{\partial t}\Lambda = 0, \\[3mm]
[M_R] \dfrac{\partial}{\partial t} U_{R,0} + [S - S_a]V_R = 0, \\[3mm]
[M_R] \dfrac{\partial}{\partial t} U_{R,\tau} + [S_a]V_R + [P_R]^T \Lambda + \tau[M_R]U_{R,\tau} = 0, \\[3mm]
[B] \dfrac{\partial}{\partial t} V_R - [R]\left(U_{R,0} + U_{R,\tau}\right) + \tau[B_a]V_R = 0, \\[3mm]
[P_L]U_L - [P_R]\left(U_{R,0} + U_{R,\tau}\right) = 0,
\end{cases}
$$

with

$$
\begin{aligned}
\left[M_{L/R}\right]_{jk} &:= \int_{\Omega_{L/R}} \Phi_k^{L/R}(\mathbf{x})\, \Phi_j^{L/R}(\mathbf{x}) \, d\mathbf{x}, & \left[P_{L/R}\right]_{jk} &:= \int_{\Gamma} \Phi_k^{L/R}(\mathbf{x})\, \phi_j(\mathbf{x}) \, d\mathbf{x}, \\[3mm]
[B]_{jk} &:= \int_{\Omega_R} \Psi_k(\mathbf{x}) \cdot \Psi_j(\mathbf{x}) \, d\mathbf{x}, & [B_a]_{jk} &:= \int_{\Omega_R} \mathbf{a}\mathbf{a}^T \Psi_k(\mathbf{x}) \cdot \Psi_j(\mathbf{x}) \, d\mathbf{x}, \\[3mm]
[S]_{jk} &:= \int_{\Omega_R} \tilde{A}_R \Psi_k(\mathbf{x}) \cdot \nabla \Phi_j^R(\mathbf{x}) \, d\mathbf{x}, & [S_a]_{jk} &:= \int_{\Omega_R} \mathbf{a}\mathbf{a}^T \tilde{A}_R \Psi_k(\mathbf{x}) \cdot \nabla \Phi_j^R(\mathbf{x}) \, d\mathbf{x}, \\[3mm]
[R]_{jk} &:= \int_{\Omega_R} \nabla \Phi_k^R(\mathbf{x}) \cdot \Psi_j(\mathbf{x}) \, d\mathbf{x}, & [K]_{jk} &:= \int_{\Omega_L} A\nabla \Phi_k^L(\mathbf{x}) \cdot \nabla \Phi_j^L(\mathbf{x}) \, d\mathbf{x}.
\end{aligned}
$$

We consider a time discretization with constant time step Δt. For any function $F(t)$ we denote by F^n the approximation of $F(n\Delta t)$. We write a second order in time scheme using leap frog approximations of the time derivatives. The dissipative terms are discretized implicitly using average values at different time step.

$$
\begin{cases}
[M_L]\dfrac{U_L^{n+1} - 2U_L^n + U_L^{n-1}}{\Delta t^2} + [K]U_L^n - [P_L]^T\dfrac{\Lambda^{n+1} - \Lambda^{n-1}}{2\Delta t} = 0, \\[3mm]
[M_R]\dfrac{U_{R,0}^{n+1} - U_{R,0}^n}{\Delta t} + [S - S_a]V_R^{n+1/2} = 0, \\[3mm]
[M_R]\dfrac{U_{R,\tau}^{n+1} - U_{R,\tau}^n}{\Delta t} + [S_a]V_R^{n+1/2} + [P_R]^T\dfrac{\Lambda^{n+1} + \Lambda^n}{2} + \tau[M_R]\dfrac{U_{R,\tau}^{n+1} + U_{R,\tau}^n}{2} = 0, \\[3mm]
[B]\dfrac{V_R^{n+1/2} - V_R^{n-1/2}}{\Delta t} - [R]\left(U_{R,0}^n + U_{R,\tau}^n\right) + \tau[B_a]\dfrac{V_R^{n+1/2} + V_R^{n-1/2}}{2} = 0, \\[3mm]
[P_L]U_L^n - [P_R]\left(U_{R,0}^n + U_{R,\tau}^n\right) = 0.
\end{cases}
\tag{36}
$$

We present a practical algorithm for implementing the previous scheme.

Computational algorithm, step 1: Prediction.   Compute $U_{R,0}^{n+1}$, $V_R^{n+1/2}$ and the temporary variables $U_L^\star$ and $U_{R,\tau}^\star$:

$$
U_L^\star = 2U_L^n - U_L^{n-1} - \Delta t^2[M_L]^{-1}\left\{[K]U_L^n + \frac{1}{2\Delta t}[P_L]^T\Lambda^{n-1}\right\},
$$

$$
U_{R,\tau}^\star = \frac{2 - \tau\Delta t}{2 + \tau\Delta t}U_{R,\tau}^n - \frac{2\Delta t}{2 + \tau\Delta t}[M_R]^{-1}\left\{[S_a]V_R^{n+1/2} + \frac{1}{2}[P_R]^T\Lambda^n\right\}.
$$

Computational algorithm, step 2: Compute the Lagrange mutliplier.   Using the last equation of (36) we can compute Λ^{n+1}:

$$
\Lambda^{n+1} = \left[\frac{\Delta t}{2}[P_L][M_L]^{-1}[P_L]^T + \frac{\Delta t}{2 + \tau\Delta t}[P_R][M_R]^{-1}[P_R]^T\right]^{-1}\left\{[P_R]\left(U_{R,0}^{n+1} + U_{R,\tau}^\star\right) - [P_L]U_L^\star\right\}.
$$

Computational algorithm, step 3: Correction.   Compute U_L^{n+1} and $U_{R,\tau}^{n+1}$ using Λ^{n+1}:

$$
U_L^{n+1} = U_L^\star + \frac{\Delta t}{2}[M_L]^{-1}[P_L]^T\Lambda^{n+1},
$$

$$
U_{R,\tau}^{n+1} = U_{R,\tau}^\star - \frac{\Delta t}{2 + \tau\Delta t}[M_R]^{-1}[P_R]^T\Lambda^{n+1}.
$$

Remark 5
The treatment of corner regions raises numerical difficulties when one uses the natural nodal trace space to discretize the lagrangian multipliers. This problem is related to the domain decomposition method and has been treated by other authors [11, 12].

5. NUMERICAL RESULTS

The numerical results presented below have been obtained using high-order spectral elements on hexahedral meshes. This technique provides good approximation properties as well as good performances as it yields mass lumping (see [14], [18]). We chose 6th order finite elements in the physical domain to ensure an accurate approximation of the continuous problem, 1st, 4th and 6th orders finite elements in the absorbing layers to emphasize the benefit of high-order discretization regarding to absorption and reflection properties. The difference of orders between physical and absorbing domains is handled by the mortar elements.

5.1. Perfectly matched layers for 2D rectangular domain

We consider the anisotropic acoustic equation (1) in a square of length 20 (Ω_φ) centered in **0** with

$$A = \left[\begin{array}{cc} 1.5 & 0.8 \\ 0.8 & 1.5 \end{array} \right]. \tag{37}$$

The volumic source is chosen of the form

$$f(\mathbf{x}, t) = 5e^{-R|\mathbf{x}|} \left[2C(f_0 t - 1)^2 - 1 \right] e^{-C(f_0 t - 1)^2}, \tag{38}$$

with $C = \pi^2$, $R = 2$, $f_0 = 2.4$. The absorption coefficient τ (in equation (21)) is chosen to satisfy

$$\tau = \tau_0 / L$$

where L stands for the width of the PML and τ_0 for a reference absorption. The overall domain is meshed using a regular grid of size $h = 0.5$ when 4th or 6th orders finite elements are used in the absorbing layers. A grid of size $h = 0.05$ is used in the absorbing layers when first order elements are chosen.

Reference computation and computations without absorption. To illustrate the basic idea behind the construction of PML for anisotropic media we present in Figure 3 different snapshots of the solution u computed with no absorption ($\tau_0 = 0$) in a large domain ($L = 20$) with 6th order finite elements. The propagating waves satisfy equations (7, 8) in the domain surrounding the physical medium Ω_φ. The corresponding complex media $\tilde{A}$ are given by table I, they are computed using the results of section 3.2 and 3.4. The reference solution u_{ref} has been computed using the reference medium A given by (37) in all layers. The resulting relative L^∞ error in time for $t \in [0, 24]$ and L^2 error in Ω_φ is $1.44e{-}07$. This value represents the maximum accuracy one can expect, with the chosen discretization, after introducing some dissipation in the media (i.e. after choosing $\tau_0 > 0$).
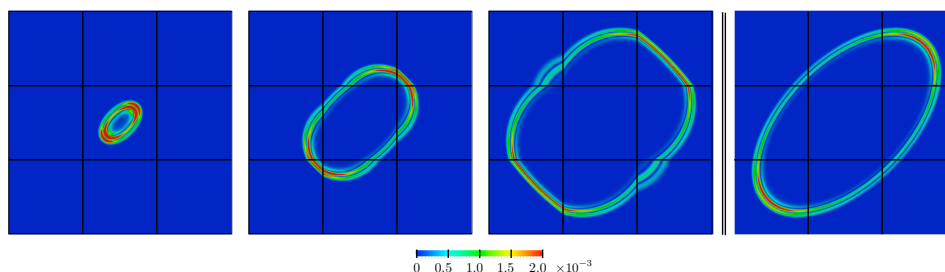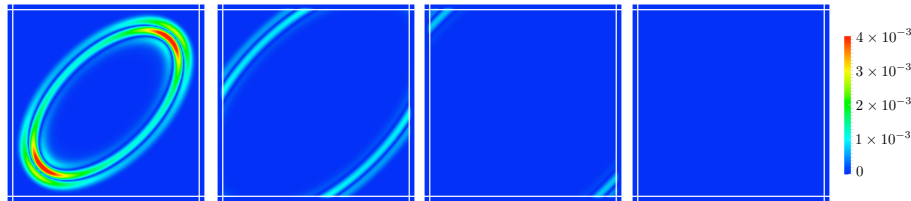

Figure 3. Left: snapshots at time $t = 4, 12, 20$ of the absolute value of the solution computed with $\tau_0 = 0$ and $L = 40$. Right: snapshot at $t = 20$ of the reference solution u_{ref} computed in a large domain $L = 40$.

A_C	A_{TB}	A_C
A_{LR}	A	A_{LR}
A_C	A_{TB}	A_C

$\tilde{A}$	$\tilde{A}\mathbf{e}_1 \cdot \mathbf{e}_1$	$\tilde{A}\mathbf{e}_2 \cdot \mathbf{e}_2$	$\tilde{A}\mathbf{e}_1 \cdot \mathbf{e}_2 = \tilde{A}\mathbf{e}_2 \cdot \mathbf{e}_1$
A_{TB}	0.86	1.5	0
A_{LR}	1.5	0.86	0
A_C	3.375/1.61	3.375/1.61	- 1.8/1.61

Table I. Perfectly matched media obtained for the different layers when $\tau = 0$.

Computations with absorption.   Figures 4 and 5 show snapshots obtained for $\tau_0 = 9$ and $L = 0.5$ with 6th order elements (i.e. there is only one layer of absorbing elements). The color scale used in figure 5 emphasizes two kinds of reflections: those due to a high absorption rate (whose wave front is nearly parallel to the interfaces) and those due to the truncation of the absorbing layer (coming form the corner), these reflections decrease by using a lower damping coefficient and adding elements in the absorbing layers.

Figure 4. Snapshots at time $t = 7, 11, 16, 20$ of the absolute value of the solution computed with $\tau_0 = 9$ and $L = 0.5$.
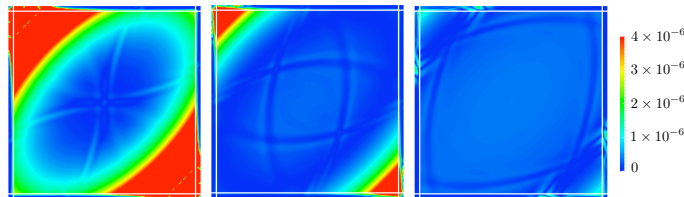
Figure 5. Snapshots at time $t = 16, 20, 24$ (color scale compressed 1000 times) of the absolute value of the solution computed with $\tau_0 = 9$ and $L = 0.5$.

Convergence results and long time behavior are given in Figure 6. The left graph represents the L^2 norm of the solution u versus time (in log-scale) inside Ω_φ for 6th order finite element with $\tau_0 = 9$ and $L = 0.5$. The right graph shows the convergence of the relative error with respect to the length of the layer, the absorption coefficient and the order of the finite elements in the PML. On the one hand, when τ is high (i.e. L is small), the reflections coming from the discretization of the perfectly matched transmission condition are predominant. This is the reason why the error is higher for $\tau_0 = 11$ compared to $\tau_0 = 7$ when $L = 0.5$. On the other hand, when τ is small (i.e. L is large), the truncation of the absorbing layers produces the predominant reflections and so the error decreases as τ_0 increases. We obtain an error around $2.47e{-}07$ in the most favorable case (highest-order functions, highest reference absorption coefficient and widest layers), which is close to the error obtained when $\tau_0 = 0$.
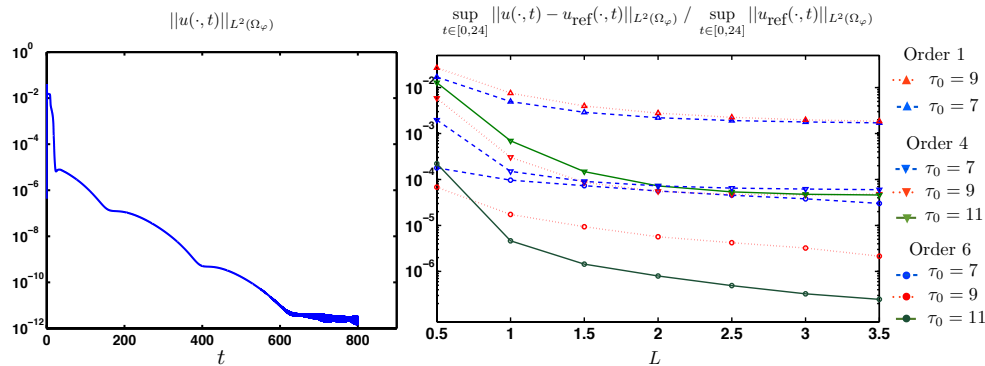

Figure 6. Left: Long time behavior of the solution (6th order finite element, $\tau_0 = 9$ and $L = 0.5$). Right: convergence of the relative error.

5.2. Perfectly matched layer for 2D convex polygonal domain

We now consider a convex polygonal domain with

$$A = \left[\begin{array}{cc} 1.5 & 0.8 \\ 0.8 & 1.3 \end{array} \right]$$

and the source defined by (38). The shape of the domain and details of the mesh are given in figure 7. The overall domain is meshed using 1521 elements and 6th orders finite elements. The absorbing layers in the edge regions are meshed using a regular grid of size $h = 0.5$ with either 4th or 6th orders finite elements. The physical mesh and the mesh in the absorbing layers are non conform. Again we define the absorption coefficient through the relation $\tau = \tau_0/L$ where L stands for the width of the PML and τ_0 for a reference absorption.
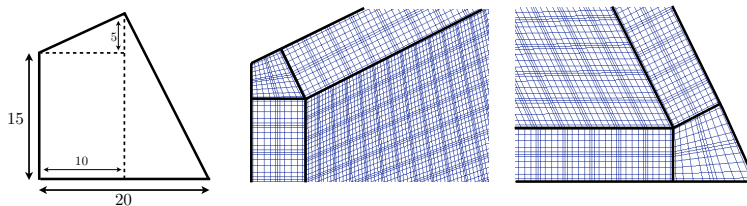
Figure 7. Left: geometry of the convex polygonal domain. Right: details of the mesh (when $L = 1$), the blue lines correspond to the sub-mesh obtained by linking the 6th order degrees of freedom (there are two layers of absorbing elements here).

Remark that there is some leeway in the choice of the geometry of the corner, the only restriction, mentioned in section 2.4, being that the surrounding layers have orthogonal boundaries (see [9] for a different geometrical construction in the case of isotropic acoustic).

Reference computation and computations without absorption. We set $\tau_0 = 0$, $L = 20$ and use 6th order finite elements. Snapshots of the solution obtained with such layers are given in figure 8 and details of the complex media $\widetilde{A}$ used in the layers are given in table II. They are computed using the results of section 3.2 and 3.3. The reference solution has been computed using the reference medium A in all layers. The resulting relative L^∞ error in time and L^2 error in Ω_φ is $1.34e{-}5$, which represents the maximum accuracy one can expect when dissipation occurs.
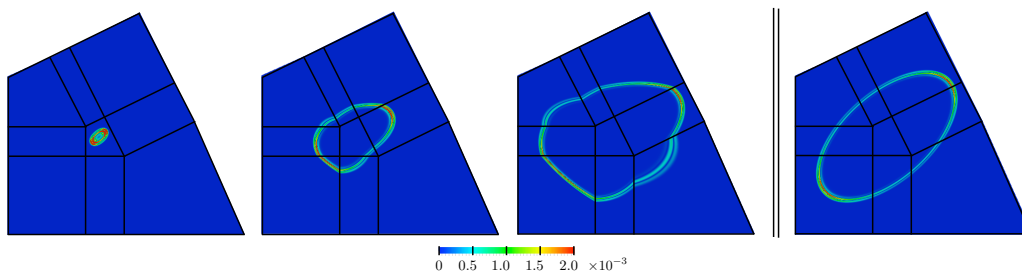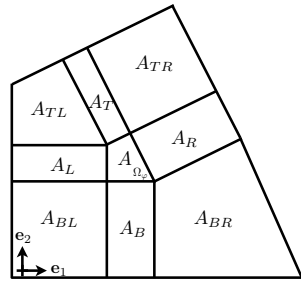

Figure 8. Left: snapshots at time $t = 3.2, 16, 28.8$ of the absolute value of the solution computed with $\tau_0 = 0$ and $L = 40$. Right: snapshot at $t = 20$ of the reference solution u_{ref} computed in a large domain $L = 40$.

$\tilde{A}$	$\tilde{A}\mathbf{e}_1 \cdot \mathbf{e}_1$	$\tilde{A}\mathbf{e}_2 \cdot \mathbf{e}_2$	$\tilde{A}\mathbf{e}_1 \cdot \mathbf{e}_2 = \tilde{A}\mathbf{e}_2 \cdot \mathbf{e}_1$
A_B	1.007692	1.3	0
A_L	1.5	0.873333	0
A_R	1.804762	0.919048	0.590476
A_T	1.637143	0.934286	0.468571
A_{BR}	4.376336	1.458779	-0.833588
A_{TL}	1.683206	0.561069	-0.320611
A_{BL}	2.232824	1.935115	-1.190840
A_{TR}	2.401374	0.740611	0.359084

Table II. Perfectly matched media obtained for the different layers when $\tau = 0$.

Computations with absorption.   Figures 9 and 10 show snapshots obtained for $\tau_0 = 9$ and $L = 1$ with 6th order elements (i.e. there are only two layers of absorbing elements). The reflections due to the truncation of the absorbing layer (coming form the corner) is predominant but decreases when L increases as shown by the convergence graph given in figure 6. The long time behavior of the solution is plotted Figure 6.
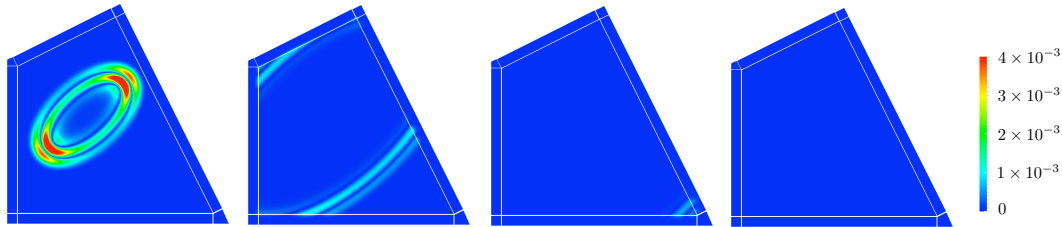
Figure 9. Snapshots at time $t = 4, 10.4, 20, 24$ (color scale compressed 1000 times) of the absolute value of the solution computed with $\tau_0 = 9$ and $L = 1.0$.
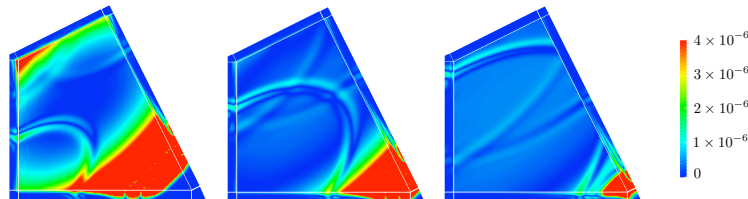
Figure 10. Snapshots at time $t = 16, 20, 24$ (color scale compressed 1000 times) of the absolute value of the solution computed with $\tau_0 = 9$ and $L = 1.0$.

The convergence of the relative error when 4th order finite elements are used illustrates well the phenomenon described in the rectangular case. When τ is high, i.e. small L, the reflections coming from the discretization of the perfectly matched transmission condition are predominant while for low τ, i.e. large L, the truncation of the absorbing layers produces the predominant reflections and so the error decreases as τ_0 increases. For both orders of finite elements the relative error decreases to a minimum around $8.84e-5$ when τ_0 and L increase. The minimum is reached with the highest-order functions, highest reference absorption coefficient and widest layers and is close to the relative error obtained when $\tau_0 = 0$.
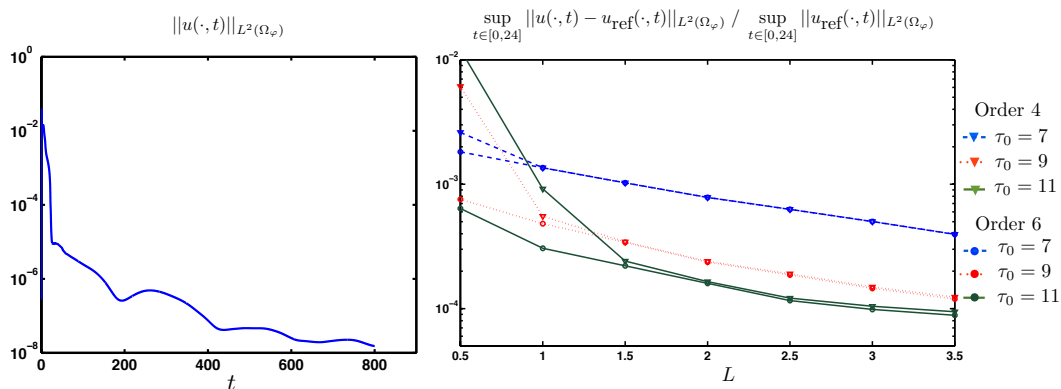
Figure 11. Left: Long time behavior of the solution (6th order finite element, $\tau_0 = 9$ and $L = 1$). Right: convergence of the relative error.

5.3. Propagation in 3D rectangular domain

Our final example concerns a 3D anisotropic acoustic case in a cube of length 10 with

$$A = \begin{bmatrix} 1.6 & 0.8 & 0.6 \\ 0.8 & 1.4 & 0.4 \\ 0.6 & 0.4 & 1.2 \end{bmatrix}.$$

We use the source defined by (38) with $C = 5\pi^2$, $R = 20$ and $f_0 = 0.4$, a regular grid of size $h = 0.5$, 6th order finite elements and one layer of elements in the PML. We have 1,771,561 degrees of freedom in the physical domain and 688,778 in the PML. 59.5% of the computational time was spent for the propagation in the physical domain, 32.5% for the propagation inside the absorbing layers. Finally 5% of the computational time was spent to treat the transmission condition and 3% to treat the computation of the source. Snapshots of the numerical results are presented figures (12,13,14).
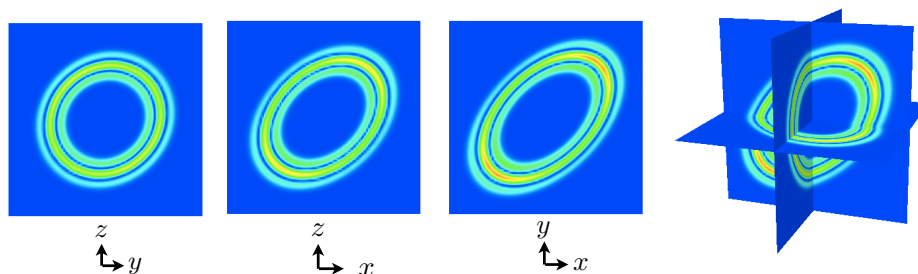

Figure 12. Snapshots at time $t = 5.35$ (color scale compressed 1000 times) of the absolute value of the solution.

6. CONCLUSION

Sufficient criteria for the existence of solutions without parasitic reflections have been given for particular transmission problems between the physical domain and an absorbing layer. These criteria have been extended to corner regions. Then a generalization of the stability criteria introduced in [8] has been proved for the time domain problem. Perfectly matched layers for anisotropic acoustic problems in convex polygonal media have been derived and a numerical algorithm that uses high order finite elements together with mortar elements has been introduced. A constant
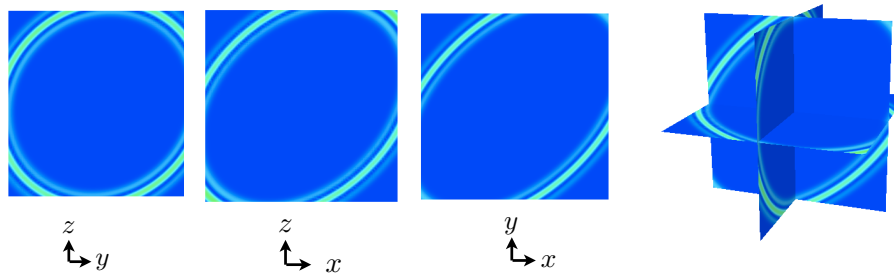
Figure 13. Snapshots at time $t = 10.79$ (color scale compressed 1000 times) of the absolute value of the solution.
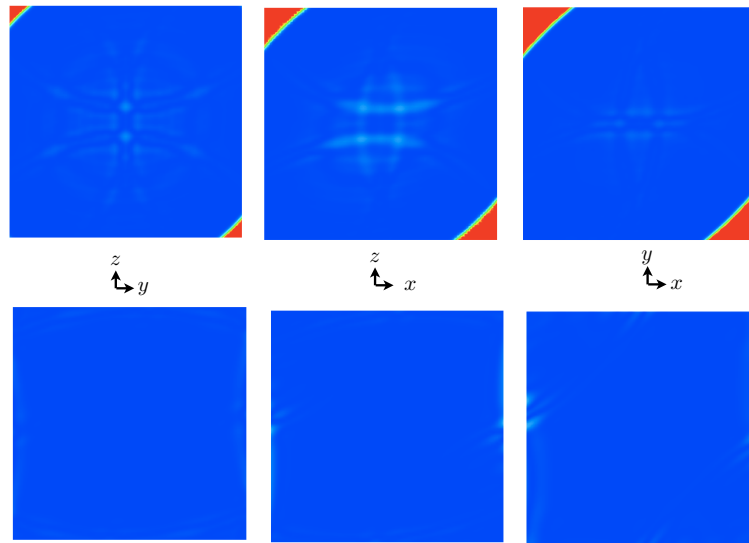

Figure 14. Snapshots (color scale compressed 1000 times) at time $t = 10.79$ (top) and $t = 16.19$ (bottom) of the absolute value of the solution, in the plane $x = 0$, $y = 0$, $z = 0$ respectively.

damping function has been used in the layers to reduce the width of the PML and to simplify the discretization process. Convergence results in 2D confirm the validity of our approach. The optimization of the profile of the damping function, of the width of the PML and of the order of the finite element approximation will be the subject of further studies. Moreover, beyond these applications we hope this study will lead to a better knowledge of the construction of absorbing layers for arbitrary anisotropic elastodynamics.

REFERENCES

1. J. Berenger. A perfectly matched layer for the absorption of electromagnetic waves. *Journal of Computational Physics*, 114:185–200, 1994.
2. D. Komatitsch and R. Martin. An unsplit convolutional perfectly matched layer improved at grazing incidence for the seismic wave equation. *Geophysics*, 72(5):SM155, 2007.
3. P. Petropoulos, L. Zhao, and C. Cangellaris. A Reflectionless Sponge Layer Absorbing Boundary Condition for the Solution of Maxwell's Equations with High-Order Staggered Finite Difference Schemes. *Journal of Computational Physics*, 139(1):184–208, January 1998.
4. Y.F. Li and O. Bou Matar. Convolutional perfectly matched layer for elastic second-order wave equation. *Journal of Acoustical Society of America*, 127(3):1318–1327, 2010.
5. W.C. Chew and W.H. Weedon. A 3D perfectly matched medium from modified Maxwell's equations with stretched coordinates. *Microwave and Optical Technology Letters*, 7(13):599–604, 1994.
6. F. Collino and C. Tsogka. Application of the perfectly matched absorbing layer model to the linear elastodynamic problem in anisotropic heterogeneous media. *Geophysics*, 66(1):294–307, 2001.

7. J. Diaz and P. Joly. A time domain analysis of PML models in acoustics. *Computer Methods in Applied Mechanics and Engineering*, 195(29-32):3820–3853, 2006.

8. E. Becache, S. Fauqueux, and P. Joly. Stability of perfectly matched layers, group velocities and anisotropic waves. *Journal of Computational Physics*, 188:399–403, 2003.

9. M.N. Guddaty and K.-W. Lim. Continued fraction absorbing boundary conditions for convex polygonal domains. *International Journal for Numerical Methods in Engineering*, 66:949–977, 2006.

10. S. Savadatti and M.N. Guddati. Absorbing boundary conditions for scalar waves in anisotropic media. Part 2: Time-dependent modeling. *Journal of Computational Physics*, 229(18):6644–6662, September 2010.

11. A. Bendali and Y. Boubendir. Non-overlapping domain decomposition method for a nodal finite element method. *Numerische Mathematik*, 103(4):515–537, 2006.

12. M. Gander, F. Magoules, and F. Nataf. Optimized Schwarz methods without overlap for the Helmholtz equation. *SIAM Journal on Scientific Computing*, 24(1):38–60, 2003.

13. F. Nataf. A new approach to perfectly matched layers for the linearized Euler system. *Journal of Computational Physics*, 214(2):755–772, 2006.

14. G. Cohen. Higher-order numerical methods for transient wave equations. *Springer*, 2002.

15. D. Appelo, T. Hagstrom, and G. Kreiss. Perfectly matched layers for hyperbolic systems: general formulation, well-posedness, and stability. *SIAM Journal on Applied Mathematics*, 67(1):1–23, 2007.

16. H.O. Kreiss and J. Lorenz. Initial-boundary value problems and the Navier-Stokes equations. *Academic press*, 136, 1989.

17. D. Appelo and G. Kreiss. A new absorbing layer for elastic waves. *Journal of Computational Physics*, 215(2):642–660, 2006.

18. D Komatitsch and J Tromp. Introduction to the spectral element method for three-dimensional seismic wave propagation. *Geophysical Journal International*, 139(3):806–822, January 2002.